THE JOURNAL OF THE ACOUSTICAL SOCIETY OF KOREA VOL.24, NO.3E 2005. 9 pp. 90~98

Enhanced Approach Using Computational and Experimental Method for the Analysis of Loudspeaker System

Seok-Tae Park*
*Dept. of Acoustical Eng., Juseong College
(Received May 26 2005; revised July 19 2005; accepted August 8 2005)

Abstract

Enhanced approach using computational and experimental method is proposed and performed to describe very well the behavior of loudspeaker than conventional method. Proposed procedure is composed of four parts. First, Thiele-Small parameters for test loudspeaker are identified by an electrical impedance method like as a delta mass method. Second part includes the processes to measure physical properties. Physical data like masses and thicknesses of loudspeaker's components are measured by an electrical precision scale and a digital vernier caliper. Third, the identified Thiele-Small parameters are proposed to be used as load boundary conditions for vibration analysis instead of electromagnetic circuit analysis to get a driving force upon bobbin part. Also, these parameters and physical data are used to modify physical properties required for computation to accommodate simulated sound pressure level with measured one for loudspeaker enclosure system. These data like as Young's modulus and thickness for a diaphragm are required for vibration analysis of loudspeaker but not measured accurately. Finally, it was investigated that simulated sound pressure level with full acoustic modeling including an acoustic port for test loudspeaker agreed with experimental result very well in the midrange frequency band(from 100 Hz to 2,000 Hz). In addition, several design parametric study is performed to grasp acoustical behaviors of loudspeaker system due to variations of diaphragm thicknesses and shapes of dust cap.

Keywords: *Loudspeaker, Thiele-Small Parameters, Finite Element Method, Acoustic Boundary Element Method, Loudspeaker Acoustic Radiation*

I. Introduction

Dynamic loudspeaker is a compound system that is composed of electrical, mechanical and acoustical one. Moreover, it is regarded as a sort of transducer, which transforms electrical signals to acoustical ones. In order to enhance the sound quality and to get the high power efficiency for loudspeaker, many researchers have endeavored to develop new design techniques and methodologies for loudspeaker's components. Especially, to get the high sound power researchers have focused on adopting new materials and embodying optimal magnetic circuit for motor driving part. Magnetic circuit optimizations are dependent on the choice of materials with high permeability and geometrical alignments like as heights of voice coil and front plate. Moreover, researchers have developed surface coating treatment and shape optimization for diaphragm of mechanical part. In view of theoretical approaches to loudspeaker, Beranek[1] studied

Corresponding author: Seok-Tae Park (stpark@jsc.ac.kr)
Department of Acoustical Engineering, Juseong College. SATIC, 203-31, Naeduck-dong, Sangdang-gu,Choengju-si, Chungbuk-do, 360-805, Korea

analytical model of loudspeaker and proposed equivalent electrical circuit for unified analysis. Olson[2] modeled suspension of loudspeaker as three order terms of displacement and nonlinear compliance of enclosure box with air spring as two order terms of displacement. He also developed suspension with accordion shape to reduce nonlinear characteristics of surround and spider due to large excursion. Ashley[3] presented identification programs for Thiele-Small (T-S) parameters written by BASIC and FORTRAN codes. Kaizer[4] modeled nonlinear characteristics of loudspeaker using Volterra series expansion and compared simulated results with measured ones. Klippel[5] identified nonlinear parameters of loudspeaker based on Kaizer's research. Jang[6] modeled nonlinear characteristics of loudspeaker as a black box model using nonlinear autoregressive moving average with exogenous input and Jeung[7] identified nonlinear parameters by harmonic balance method. Park[8] proposed two-stage harmonic balance method to identify nonlinear parameters of loudspeaker and adopted higher order frequency response functions to analyze nonlinear characteristics of loudspeaker in frequency domain. In computational approaches to loudspeaker, Frankort[9] modeled loudspeaker as a spring-mass lumped system and presented vibration patterns and radiation behaviors for loudspeaker. Kaizer[10] calculated acoustic radiations of loudspeaker by using finite element method (FEM). Porter[11] studied diffraction analysis for loudspeaker enclosure cabinet by geometric optical method. Kim[12,13] performed acoustic analysis for loudspeaker with ported enclosure by using boundary element method (BEM) and in that case, to input data for computational analysis, he measured physical and material properties like as Young's modulus and density.

In this paper, it is proposed to use data obtained by T-S parameters identification methods for computational analysis. It is also proposed to modify inaccurate material and physical properties that are Young's moduli and thicknesses by comparing computational results and experimental ones. In addition, it is proposed and discussed which types of loudspeaker model are more adequate to describe the on-axis acoustic radiation curves for the loudspeaker system with enclosure. That is, three BEM models for loudspeaker enclosure are presented and their on-axis acoustic radiation curves are calculated by BEM. Optimal BEM model for loudspeaker enclosure are determined by comparing simulated results and experimental one. Moreover, it discusses acoustic pressure predictions according to variation of thicknesses and shapes for diaphragm assembly.

This paper consists of four parts. First part is to identify T-S parameters for test loudspeaker unit. Added (or delta) mass method is used to identify T-S parameters. Two electrical impedance curves are required for this method. Electrical impedance curve for test loudspeaker is first measured on free air condition and then, loudspeaker is excited by constant driving voltage from 10Hz to 40,000Hz. Second impedance curve is measured with known mass attached to loudspeaker's dust cap. T-S parameters are identified with these two impedance curves by a delta mass method. Several parameters are identified like as, mass of diaphragm assembly including diaphragm, dust cap, suspension, former, voice coil and spider, fundamental resonant frequency, and force factor Bl, magnetic flux density * voice coil length. Second part is to measure physical properties of loudspeaker's components. In this part, loudspeaker is broken up as its components. Mass of suspension, diaphragm, dust cap, spider, former and voice coil is measured respectively by an electrical precision scale, AND co., model HM-202, range up to 200g, resolution 0.1mg. Geometric dimensions like as thicknesses, diameters, and lengths of loudspeaker's components are measured by a digital vernier caliper. However, it is questionable for thicknesses of each component to be accurately measured because each component is very thin and soft, and thus when it is pressed by a caliper, its thickness may be changed due to pressure. Third part is vibration analysis of loudspeaker unit by FEM. In FE modeling for loudspeaker unit, mass of each component is calculated as area * thickness * density of each component. Each simulated mass by FEM is compared with one measured in second part. Compared simulated mass with test one, thickness of each component required for FEM analysis is modified correctly on that part. Vibration analysis for loudspeaker is conducted for two purposes. One is to calculate natural resonant frequencies of loudspeaker and the other one is to obtain displacements at nodes of diaphragm surface excited by constant voltage driving force to bobbin. Now, it is proposed for Young's modulus of suspension to be modified correctly as followed by trial and error method. Fundamental resonant frequency of loudspeaker which is identified by a delta mass method in part one is compared with one obtained by FEM as in part three, in which it assumes Young's modulus. Therefore, Young's modulus is modified by iterative processes in order to fit simulated fundamental resonant frequency of loudspeaker with experimental one. In part three, three FEM vibration models for test loudspeaker are considered to provide more realistic boundary conditions for acoustic BEM analysis for loudspeaker enclosure system. Fourth part deals with acoustic analysis for loudspeaker enclosure by using BEM. Three

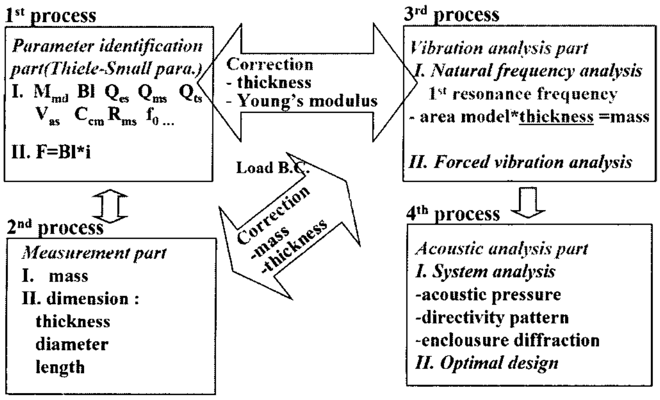

Figure 1. Proposed analysis process for loudspeaker design.

BEM models are simulated and their acoustic response functions are compared with measured result, and the best acoustic BEM model for loudspeaker enclosure is regarded as one approximately similar to measured one. Figure 1 depicts the full procedures, which will be discussed in this paper.

II. Physical data extraction and modeling of loudspeaker

In this paper, the basic data for test loudspeaker model SE8SR (nominal impedance 8 Ohm, diameter 8 inch) are obtained by identifying T-S parameters using a delta mass method based on two electrical impedance curves[14-16]. Loudspeaker is modeled as an equivalent electrical impedance type as in Figure 2. In Figure 2, Revc means pure voice coil resistance at dc, 0Hz and motor element consists of two components with frequency dependence, Rem and Lem to fit impedance rising at high frequency of voice coil. Motor impedance is represented as equation (3).

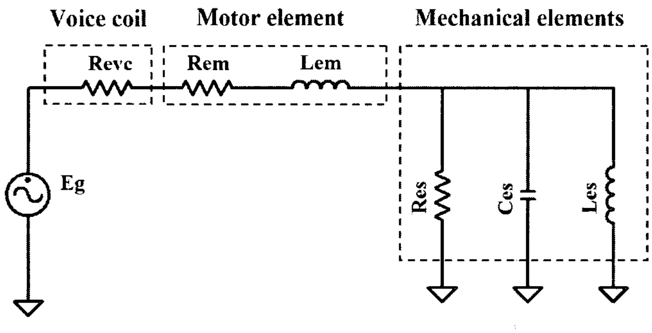

Figure 2. Electrical analogy circuit for loudspeaker unit.

$$R_{em} = R_{em}(\omega, K_{rm}, E_{rm}) = K_{rm}\omega^{E_{rm}} \quad (1)$$

$$L_{em} = L_{em}(\omega, K_{xm}, E_{xm}) = K_{xm}\omega^{E_{xm}-1} \quad (2)$$

$$Z_{em} = R_{em} + j\omega L_{em} = K_{rm}\omega^{E_{rm}} + j\omega K_{xm}\omega^{E_{xm}} \quad (3)$$

Where, Krm, Erm, Kxm, Exm is constant and ω is 2π *frequency.

To identify T-S parameters by a delta mass method, impedance measurements must perform two times. One is measured on free air condition and another is measured on an added mass attached on dust cap with known mass. In Figure 3, abscissa axis means frequency axis and ordinate axis means magnitude of electrical impedance for test loudspeaker. Solid line shows free air impedance curve and dashed line means impedance one with an added mass, which a fundamental resonant frequency shifts to left due to mass increase. Maximum magnitude of impedance is occurred at a resonant frequency. Ratio r_0 at maximum impedance is related with Re and Res. Ratio r_1 is determined at half power points, f_1 and f_2 frequency of impedance curve. T-S parameters are listed in Table 1. LEAP (Loudspeaker Enclosure Analysis Program) software is used to identify T-S parameters. It shows fundamental resonant frequency of loudspeaker F_0, 65 Hz. This value is used to modify Young's modulus of suspension part, which will be modeled in FEM for vibration analysis. In addition, diaphragm assembly mass, Mmd, is 18.7 grams and this data is utilized to correct thickness of diaphragm assembly. Mmd represents an equivalent mechanical mass of diaphragm assembly including mass for diaphragm, surround, spider and bobbin and voice coil and air load. Sensitivity value of test loudspeaker shows 95.8dB. Cms, which means 1/spring coefficient, is a mechanical compliance of driver suspension due to suspension and spider.

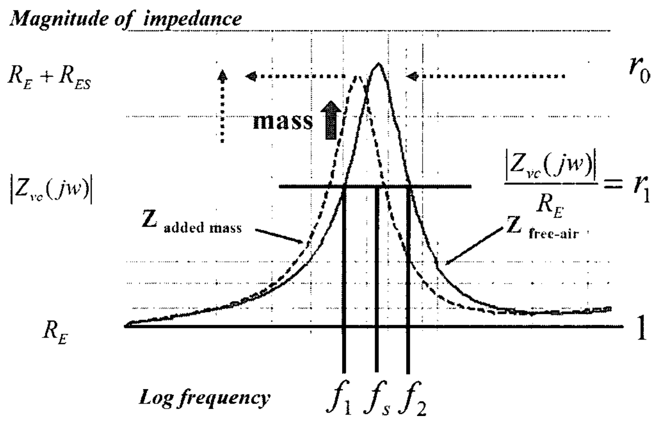

Figure 3. Comparison of driver voice coil impedance for loudspeaker; solid line, free air condition; dashed line, delta mass condition.

Table 1. Thiele-Small parameters for a test loudspeaker model SE8SR.

Name	Symbol, units	Identified results
Nominal rated impedance	Znom, Ohm	8.000
DC voice coil resistance	Revc, Ohm	5.700
Resistance constant of the motor impedance	Krm, mOhm	19.792
Reactance constant of the motor impedance	Kxm, mH	14.095
High frequency slope exponent of the motor resistance	Erm	0.596
High frequency slope exponent of the motor reactance	Exm	0.690
Equivalent acoustic diaphragm area	Sd, m2	0.0260
Electromagnetic strength	Bl, Tm	11.9126
Equivalent acoustic volume of the transducer	Vas, liter	27.0773
Equivalent mechanical compliance of the transducer	Cms, um/N	282.0728
Equivalent total mechanical moving mass of the transducer	Mms, g	21.1304
Physical mass of the diaphragm part without air load	Mmd, g	18.7198
Resonance frequency of the diaphragm and suspension at baffle	Fi, Hz	61.763
Resonance frequency of the diaphragm and suspension at free air	Fo, Hz	65.191
Mechanical losses in the suspension	Qms,	7.173
Electrical losses in the voice coil	Qes,	0.348
Total losses in the transducer	Qts,	0.332
Nominal rated power of the transducer	Pmax, W	300.00
Height of the voice coil winding	Hvc, mm	9.180
Height of the magnetic field gap	Hag, mm	3.000
Overhang or under hang of the coil outside or inside the gap	Xmax, mm	3.090
Theoretical sensitivity in dBspl	SPLo, dB	95.23
Conversion efficiency in % from electrical to acoustical energy	η_o , %	2.09

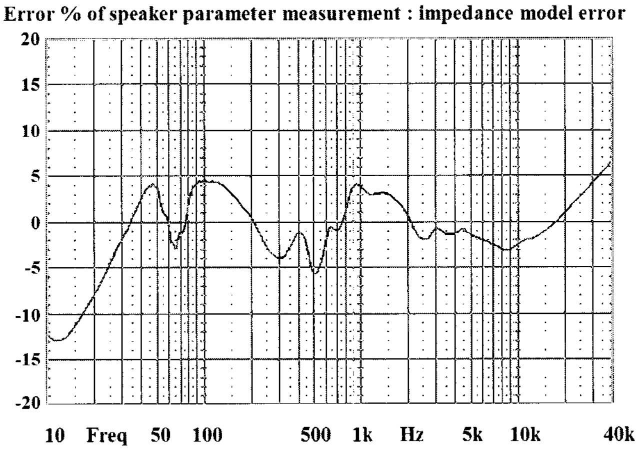

Figure 4. Error %(f) curve for electrical impedance curve based on experimental electrical impedance curve and simulated one by T-S parameters.

Figure 4 shows error % curve, which is calculated from measured impedance curve and simulated one based on identified T-S parameters by LEAP. Between 20Hz and 30 kHz frequency range, error % is between -5% and +5%. Thus, T-S parameters are well identified to describe the behavior of test loudspeaker[15]. Force factor Bl, 11.9 Tesla-meter, is used to calculate excitation force Bl*current flow in forced vibration analysis according to frequencies. That is, Bl * i is used to excite loudspeaker's bobbin. In this paper, it is proposed to use this simulated force to excite loudspeaker. Current i is simulated by using LEAP software when one-watt power is excited to test loudspeaker. Figure 5 shows magnitude and phase curve of current flowing in voice coil. Lower curve is the phase plot of current. Upper curve shows the magnitude of current and dip near 65Hz shows due to a mechanical resonance. Excitation forces to bobbin are applied at 1/3 octave center frequencies to calculate diaphragm displacement on forced vibration analysis using FEM. Masses and thicknesses for diaphragm, surround, spider and bobbin (former) are measured by an digital electrical precision scale. Masses for each component in loudspeaker FE model are respectively calculated from thicknesses and volumes simulated by FEM software as in third process in Figure 1. Thicknesses are modified by comparing simulated masses and measured ones by an electrical precision scale. Exciting force, Bl*i, is used to excite loudspeaker for FEM analysis as a load boundary condition.

Young's modulus for each component of loudspeaker is the basic data for FE computational analysis. However, Young' modulus can not be measured because the test specimen obtained from dust cap and diaphragm and surround are extracted from test loudspeaker but they are too long to admit test jig insertion

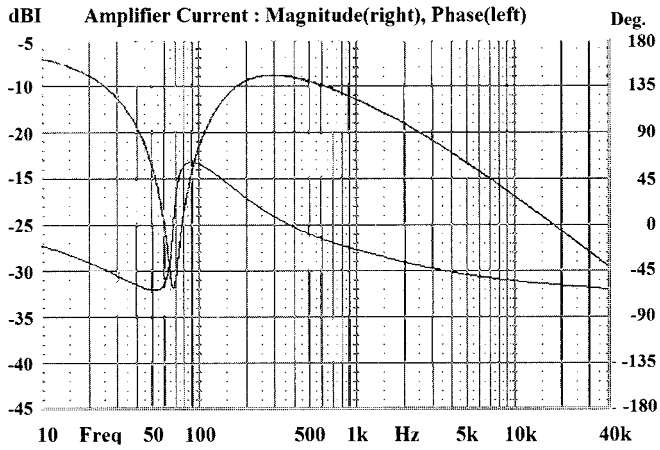

Figure 5. Load boundary condition, simulated current by LEAP software.

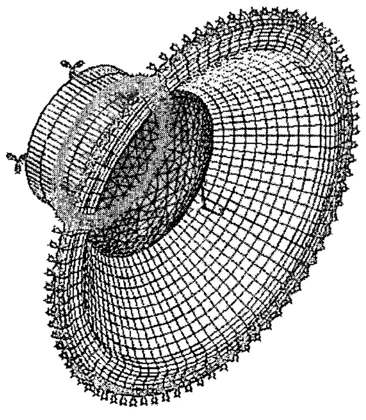

Figure 6. FEM model I for loudspeaker.

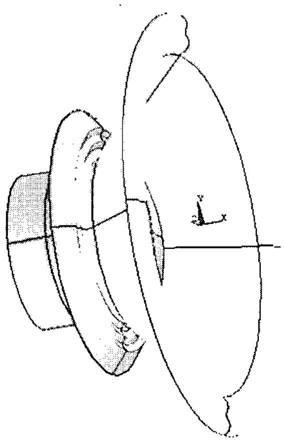

Figure 7. FEM model II for loudspeaker, area model.

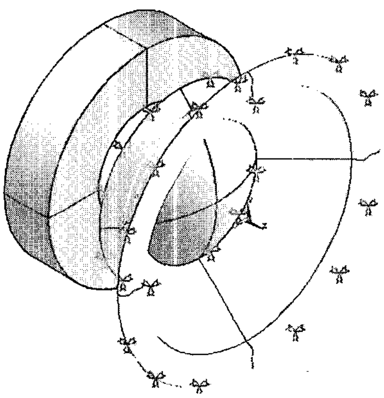

Figure 8. FEM model III for loudspeaker, area model.

for tensile test. It occurs slip phenomena in fixture during tensile test and cannot get correct Young's modulus. To overcome this drawback, in this paper, it is proposed that Young's modulus for surround component is determined by fitting simulated fundamental resonant frequency by FEM to F_0 in T-S parameters as in third process in Figure 1. In proposed method, Young's modulus is an equivalent dynamic value not static one by a tensile test. Therefore, it may be thought that a dynamic behavior of test loudspeaker can be described more realistic than using static Young's modulus obtained by tensile test. By the way, first fore and aft resonant motion is determined by lumped mass and equivalent stiffness of diaphragm system. Mass of diaphragm system is consisted of the sum of mass of diaphragm, dust cap, bobbin, voice coil, surround and spider and air load. Total mass and stiffness of loudspeaker system are easily obtained and but it is difficult to calculate each contribution over total equivalent stiffness at first resonant frequency, and in this paper it assumes that stiffness ratio of suspension and spider is 1 to 4. To choose the best model for Young's modulus of diaphragm three loudspeaker models are considered and analyzed[14, 17]. First model considers a simple diaphragm which do not consider spider part (Figure 6) but total stiffness of system is equivalent to the sum of surround' stiffness and four pseudo springs attached at the end surface of bobbin part to compensate spider's stiffness. Second one is more plausible model including spider part (Figure 7) and spider is modeled by shell elements. Third one is modeled for the purpose of boundary element method (BEM) analysis, which includes modeling of pole piece port for BEM, which give the acoustic duct effects, and vibration FEM analysis for diaphragm part is performed for the same shape as the second FE model. Therefore, vibration results are the same as the second model of diaphragm (Figure 8).

III. Vibration finite element analysis for loudspeaker

FEM model for the first model is composed of 2,405 nodes (dust cap, 485 nodes; surround part, 880 nodes; diaphragm, 1040 nodes; and bobbin, 400 nodes) and 2,644, shell 63, elements (dust cap, 564; surround part, 800; diaphragm, 960; and bobbin, 320 elements)[14,17]. Vibration FEM analysis for these three cases are performed respectively at 1/3 octave center frequencies in audio frequency band. In addition, resultant velocity distribution data on nodal points of diaphragm are used as velocity boundary condition for acoustic uncoupled BEM analysis[12]. Figure 9 shows several resonant modes for loudspeaker FE model I after natural frequency analysis. First mode shows fore and aft motion. Various patterns of vibration modes are obtained and these results are used to judge the effects of vibration characteristics due to variation of the thickness and Young's modulus and shapes of loudspeaker's components. Forced vibration analysis for this simple model are performed and the results are the displacement on nodes of loudspeaker at the 1/3

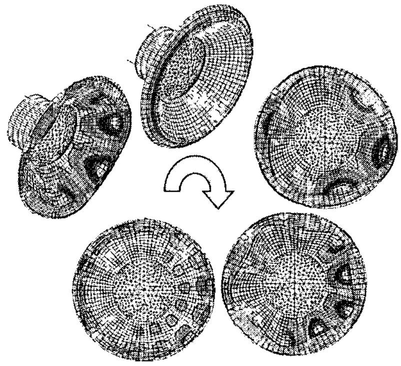

Figure 9. Vibration resonance modes of model I, simple model; first mode-upper center, higher modes -clockwise

octave center frequencies from 31.5Hz to 20,000Hz. Of course, results over 8,000Hz are meaningless but are left to compare with experimental ones. The amounts of vibration FE analysis data for test loudspeaker are required about 400MB disk space and these data are transferred and used to velocity boundary conditions (VBC) for acoustic BEM analysis. However, acoustic results for this simple model I which use VBC obtained from the first FEM model shows no good agreements with test results (refer to Fig.14) and therefore the second FE model for loudspeaker is considered.

IV. Acoustic boundary element analysis for enclosure box

An enclosure box that is installed a test loudspeaker at center position, net volume of 98 liters is used for BEM analysis and experiment. BEM model for diaphragm system and enclosure is consisted of 1,609 nodes and 1,786 elements for the first BEM case. Mesh size of loudspeaker for BEM analysis is larger than one for FEM analysis and therefore calculation time is shorter than using same size model used in FEM analysis. Maximum length of BEM elements for loudspeaker part is 7mm and therefore effective upper frequency limit for BEM analysis is 8,000Hz according to 1/6 wave length rule[13,18]. Figure 10 shows the section view for the third case of BEM model. In Figure 10, a loudspeaker unit shows BEM model III (Figure 8) including air port with FEM model II.

Figure 11 shows acoustic radiation pattern of a test loudspeaker for the BEM model I at 1,250Hz and diffraction phenomena of enclosure backwards. In Figure 11, 0 degree means on axis direction of loudspeaker. Figure 12 shows acoustic pressure distribution on surface of diaphragm of the BEM model I simulated at 1/3 octave center frequency, 1,250Hz, and it shows unique acoustic pattern on dust cap. As in the FEM model I, two other FE model cases also are considered in vibration FEM analysis and their resultant vibration data on nodes are transferred to BEM analysis and it shows which FEM model is more adequate to predict acoustic pressure patterns accurately. Consequently, acoustic BEM analysis using VBC obtained from FEM mode II, Figure 7, also shows no good results for acoustic prediction as FEM model I.

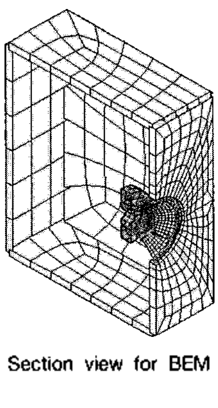

Figure 10. Section view for BEM model III.

Figure 13 shows comparison for sound pressure level (SPL) between one simulated by T-S parameters and measured one at room condition for test loudspeaker enclosure. LEAP software is used to simulate SPL but it has two major drawbacks. One is limitation of simulation space. It cannot consider room condition but free space. Another is that LEAP is based on T-S parameters and therefore higher order resonant effects of diaphragm can not be considered. Below 200Hz, measured SPL is greater than simulated one, it may be room effects. At 1 kHz, dip in curve

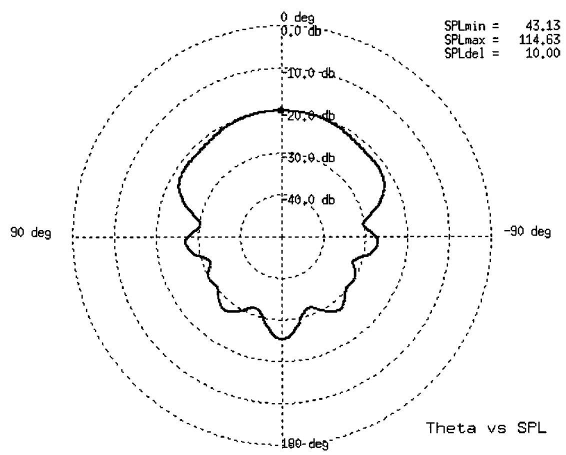

Figure 11. Acoustic pressure radiation pattern of loudspeaker enclosure at 1,250Hz.

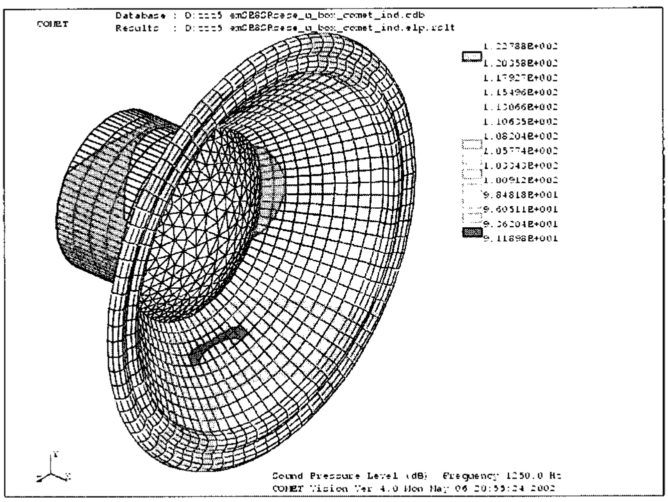

Figure 12. Acoustic pressure radiation pattern at surface of loudspeaker at 1,250Hz for model I.

means existence of sound reflections in room. Figure 14 shows SPL comparisons simulated for the three acoustic BEM models. Model III, dashed circle, is the best agreement with SPL simulated by T-S parameters. Acoustic analysis for model I is conducted with VBC based on vibration FE model I which spider part is substituted as four spring elements (dotted line with triangle mark). Stiffness coefficients for equivalent spring elements is determined to equal first resonant frequency of loudspeaker in free air, 65Hz. Model II uses FE results from FE model II. Model II includes spider part modeling but not pole piece port (dash-dot line with rectangle mark). Model III uses VBC from FE mode II (dashed line with circle mark). However, model III models spider and pole piece port. This is the different from model II for acoustic BEM analysis.

Main differences in SPL occur below 1 kHz frequency. SPL for model I show lower level than simulated one by T-S parameters in low frequency range. SPL for model II shows higher level than one for model I. Model III is similar to simulated one between 100Hz and 2 kHz frequency range. Model II, which models spider but not pole piece port, cannot consider port effects in real situation. Model II also shows higher SPL level in that region than model III which includes port effects. In Figure 14, model III shows the best fit to expect the SPL for 1 watt at 1m for enclosure box, qualitatively. Figure 15 shows acoustic pressure radiation pattern of test loudspeaker for BEM model II and model III at 1,600Hz. In Figure 15, right side is BEM model III but hides port part for comparison with model II. Their pressure radiation patterns shows very different even though at the same frequency.

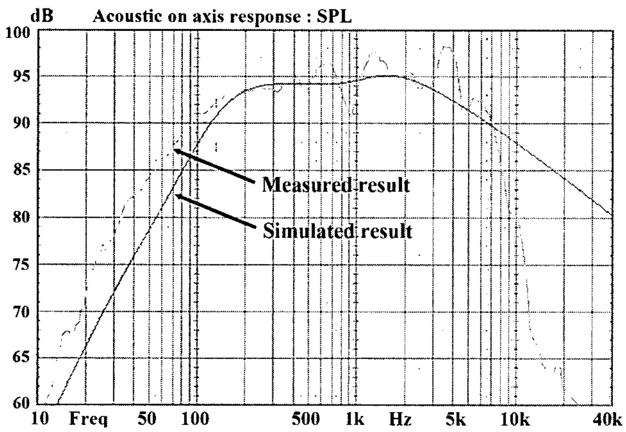

Figure 13. Comparison of SPL between measured one at room condition and simulated one by LEAP for enclosure box.

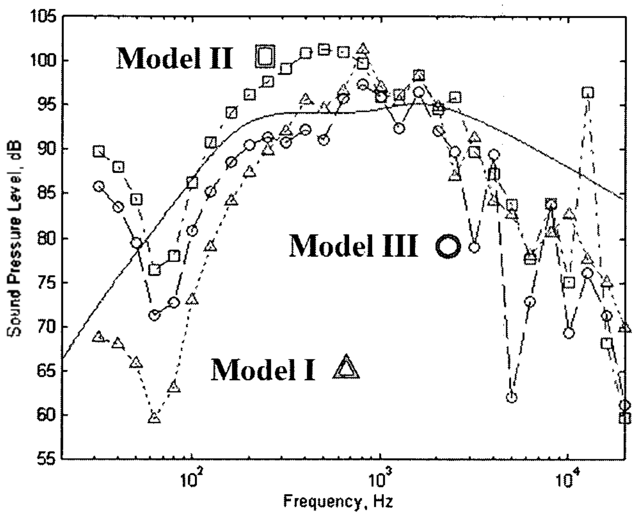

Figure 14. Comparison of on-axis SPL for loudspeaker model SE8SR of 98-liter box; solid line-simulated; dot triangle-model I; dash dot rectangle-model II; dash circle-model III.

V. Discussion on acoustic analysis according to design parameters

According to previous paragraphs, SPL for BEM model III shows the best similar to experimental result and thus design parameter study is performed on this BEM model III. In the first parametric study, acoustic effects due to thickness variations of diaphragm system are considered. Thicknesses of surround, diaphragm, and dust cap and spider part are changed like as 50% reduction, original and 100% increase. Figure 16 shows that thickness changes give rise to global change of SPL over wide frequency range but it shows distinct results that the SPL of thin case is higher than thick one at low frequency, below 500Hz. These results show mass dominated effect on SPL. Over 1 kHz, any distinct trends of SPL cannot found on original and 100%

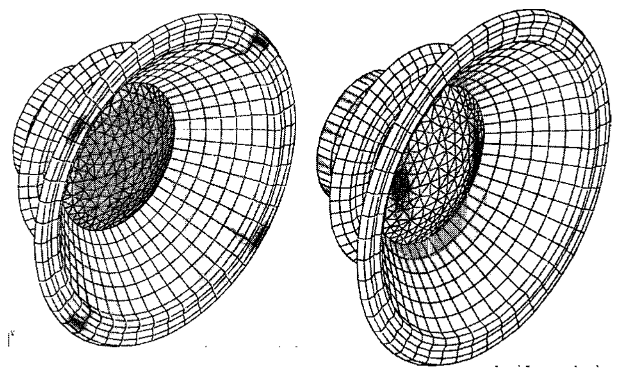

Figure 15. Acoustic pressure radiation pattern at surface of loudspeaker SE8SR; left-model II; right-model III at 1,600Hz.

increase for thickness. It can be explained as stiffness also increase due to mass increase. Second parametric study is performed on variations of dust cap shape. Figure 17 shows SPL comparisons on three cases for shape for dust cap, which is concave, flat and convex type. In lower frequency, below 500Hz, there are little differences in SPL but it shows lower SPL in convex dust cap. Moreover, up to 3 kHz flat dust cap shows more flatness of SPL but at 4 kHz sharp peak. Concave dust cap shows relatively flat SPL in mid frequency range. However, it shows complex phenomena in high frequency and this region is out of interest because sample loudspeaker is usually used below midrange frequency.

VI. Conclusions

Acoustic BEM analysis of loudspeaker was performed on three steps. First, basic physical data on loudspeaker were obtained for computation analysis by an electrical impedance (delta mass) method and compared with geometrical and physical measurements. And it was proposed that accurate values for test loudspeaker component's thickness and Young's modulus were obtained and used for computational analysis. Second, vibration displacements at nodes of diaphragm were simulated at 1/3 octave center frequencies in audio frequency band by using commercial FEM software, which used these modified input data. Finally, uncoupled acoustic BEM analysis were conducted using VBC obtained from three FE models for test loudspeaker which was installed on enclosure box, respectively. SPL simulated from three BEM models were compared with experimental result and from these results full loudspeaker model including pole piece port was the best one to simulate SPL for loudspeaker enclosure system. Additionally, it was proposed optimal design guide for design parameters according to variations of thicknesses of diaphragm system and dust cap shape, which was flat, concave and convex type.

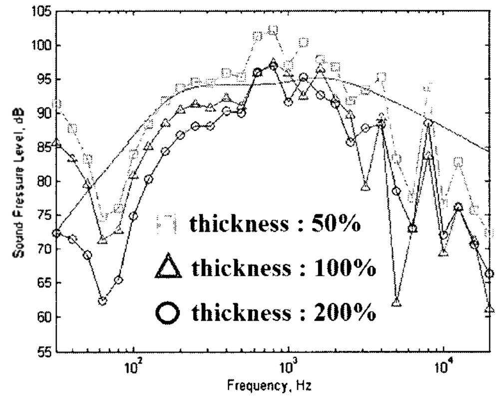

Figure 16. Comparison of on-axis SPL due to variations of diaphragm system for loudspeaker enclosure thickness @1m, 1watt.

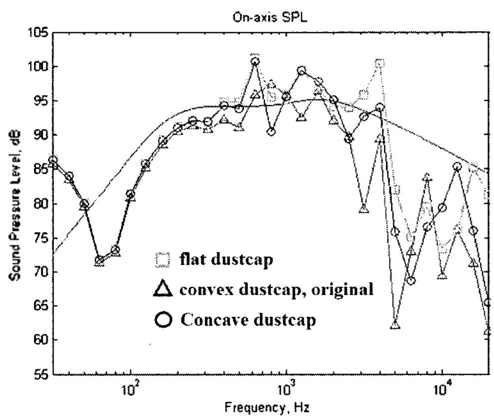

Figure 17. Comparison of on-axis SPL due to variations of shapes of dust cap for loudspeaker enclosure @1m, 1watt.

Acknowledgement

SATIC (Speaker and Audio Technology Innovation Center) funded by ministry of commerce, industry and energy has supported this work. In addition, this work is part of fundamental research on loudspeaker performed in SATIC, Juseong College, 2002.

References

1. L. L. Beranek, "Acoustics", the Acoustical Society of America, 1993
2. H. F. Olson, "Analysis of the Effects of Nonlinear Elements upon the Performance of a Back-Enclosed, Direct Radiator Loudspeaker Mechanism", Journal of Audio Engineering of Society, 10, 2, 156-162, 1962
3. J. R. Ashley and M. D. Swan, "Experimental Determination of Low-Frequency Loudspeaker Parameters", Journal of Audio Engineering of Society, 17, 5, 525-531, 1969
4. A. J. M. Kaizer, "Modeling of the Nonlinear Response of an Electrodynamic Loudspeaker by a Volterra Series Expansion", Journal of Audio Engineering of Society, 35, 6, 421-433, 1987
5. W. Klippel, "Dynamic Measurement and Interpretation of the Nonlinear Parameters of Electrodynamic Loudspeakers", Journal of Audio Engineering of Society, 38, 12, 944-955, 1990
6. H. K. Jang and K. J. Kim, "Identification of Loudspeaker Nonlinearities Using the NARMAX Modeling Technique", Journal of Audio Engineering of Society, 42, 1/2, 50-59, 1993
7. H. Jeong and J. G. Ih, "Harmonic Balance Method for Estimating the Nonlinear Parameters of Electrodynamic Direct-Radiator Loudspeakers", Journal of Audio Engineering of Society, 44, 4, 245-257, 1996
8. S. T. Park and S. Y. Hong, "Development of the Two-Stage

Harmonic Balance Method to Estimate Nonlinear Parameters of Electrodynamic Loudspeakers", Journal of Audio Engineering of Society, 49-3, 99-116, 2001
9. F. J. M. Frankort, "Vibration patterns and radiation behavior of loudspeaker cones", Journal of Audio Engineering of Society, 26 (9), 609-622, 1978
10. A. J. M. Kaizer and A. Leeuwestein, "Calculation of the Sound Radiation of a Nonrigid Loudspeaker Diaphragm Using the Finite-Element Method", Journal of Audio Engineering of Society, 36, 7/8, 948-955, 1988
11. J. Porter and E. Geddes, "Loudspeaker Cabinet Edge Diffraction", Journal of Audio Engineering of Society, 37, 11, 908-918, 1989
12. J. T. Kim, etal., "Acoustic Characteristics of a Loudspeaker Obtained by Vibroacoustic Analysis", Proceedings of the Korean Society for Noise and Vibration Engineering, 153-159, 1996
13. J. T. Kim, J. H. Kim and J. O. Kim, "Designing a loudspeaker by acoustic analysis and Taguchi method", Proceedings of the Korean Society for Noise and Vibration Engineering, 568-574, 1998
14. S. T. Park, *Study on the acoustic ration according to shapes of loudspeaker diaphragm*, Speaker and Audio Technology Innovation Center, Juseong College, fundamental research report, 2002
15. LEAP application manual, Version 4.6, Linear-X limited., 2000.
16. S. T. Park, "Study on linear parameters identification of loudspeaker", Journal of the Acoustical Society of Korea, 21 (4), 415-420, 2002
17. S. T. *Park, Analysis of loudspeaker by computational and experimental approaches*, (InterNoise2003), 602-608, 2003
18. User document, Comet Acoustics, Chapter 3 acoustic modeling, Automated Analysis Corporation, 1995

[Profile]

•Seok-Tae Park

1984.2: Hanyang Uni. (S. Korea), Dept. of mechanical engineering (B.sc)
1986.2: KAIST(S. Korea), Dept. of mechanical engineering(M.S.)
1999.2: Ajou Uni. (S. Korea), Dept. of systems engineering(Ph.D.)
1993~1999: Principal Engineer at Institute for Advanced Engineering(S. Korea)
2000.9~Present: Assistant Professor, Dept. of Acoustical Engineering of Juseong College(S. Korea).

*Main Research: the analysis and design for general speaker, microspeaker and new sound device and speaker enclosure system including car audio system.